Study on Polypropylene–Polyethylene-Based Copolymer Solidification

J. J. SUÑOL,[1] J. SAURINA,[1] P. PAGÈS,[2] F. CARRASCO[3]

[1] Department of Industrial Engineering, Universitat de Girona, Avda. Lluis Santalo, s/n E-17071 Girona, Spain

[2] Department of Materials Science, Universitat Politècnica de Catalunya, Colom 11 E-08222 Terrassa, Spain

[3] Department of Chemical Engineering, Universitat de Girona, Avda. Lluis Santalo, s/n E-17071 Girona, Spain

Received 17 December 1997; accepted 27 December 1999

ABSTRACT: In the present work, nonisothermal crystallization is analyzed. Concretely, we study the solidification process of polypropylene–polyethylene-based copolymers by means of differential scanning calorimetry (DSC). Several samples with different additives are subjected to artificial aging processes. The calculation of the specific surface energy, σ, is in good accordance with the results reported in the references. The artificial aging is responsible for a slight increase of σ values (i.e., increase of 1.6 kJ $\cdot$ m^{-2} for sample A and 0.3 kJ $\cdot$ m^{-2} for sample B). On the other hand, the σ value of sample B is considerably lower than that of samples A, C, and D (i.e., 17.3 kJ $\cdot$ m^{-2} for sample B versus an average value of 23.0 kJ $\cdot$ m^{-2} for the other samples). Microstructure analysis was performed by scanning electronic microscopy (SEM). As shown from the analysis, aging only affects superficial zones because no changes in the morphology of the central zone were detected in the different samples. Sample B shows a different behavior; it was less resistant to fracture. From DSC and SEM measurements, we can state the additive influence on the original sample behavior as well as on the solidification process of polypropylene–polyethylene-based copolymers. © 2000 John Wiley & Sons, Inc. J Appl Polym Sci 77: 1269–1274, 2000

Key words: solidification; DSC; PP–PE; artificial aging; specific surface energy

INTRODUCTION

Several studies[1–4] analyze nonisothermal crystallization kinetics. Most of methods for nonisothermal regime analysis are based on an extension of the formalism of the Avrami-Kolmogorov equation, which was first introduced to describe the transformation kinetics in the isothermal regime[5–7]:

$$\alpha(t) = 1 - \exp(-kt^n) \quad (1)$$

where $\alpha(t)$ stands for the fraction transformed for t time, k is the constant rate, and n a parameter related to the mechanisms governing the transformation. The variation of the constant rate with the temperature is generally accepted to be of the Arrhenius type,[8] because usually this relationship dominates physical and chemical phenomena.

$$k(T) = k_o\exp(-E/RT) \quad (2)$$

where k_o is the pre-exponential factor, E is the apparent activation energy, R the gas constant, and T temperature. However, Arrhenius approximation is not valid in the case of polymer crys-

Correspondence to: J. J. Suñol.

Journal of Applied Polymer Science, Vol. 77, 1269–1274 (2000)

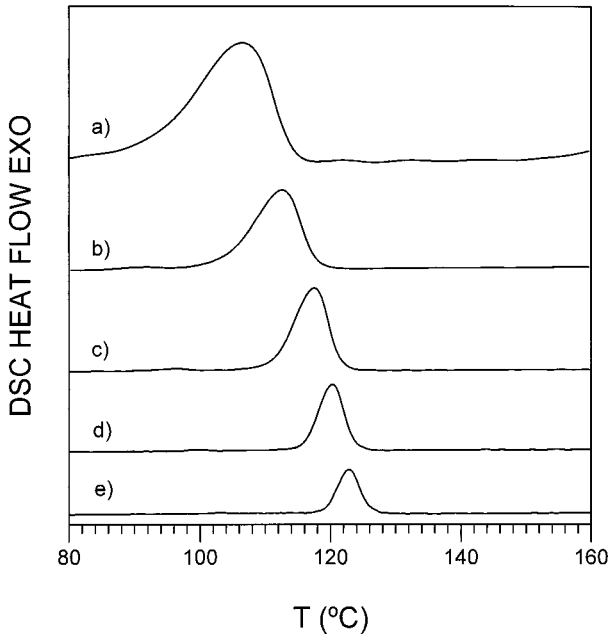

Figure 1 DSC curves corresponding to sample A cooling at different rates: (a) −40 K/min, (b) −20 K/min, (c) −10 K/min, (d) −5 K/min, and (e) −2.5 K/min.

tallization from previously molten material at relatively low rates. The reason is activation energy dependency on the cooling rate used.[9]

This work focuses on nonisothermal crystallization during cooling processes of polymeric materials. The method used is that developed by Dobreva et al.,[10,11] which consists of calculating specific surface energies.

EXPERIMENTAL

The base material was a polypropylene (PP) rich (~ 5% in weight) PP–polyethylene (PE)-based commercial copolymer (PB 140 manufactured by Repsol, Spain) incorporating several different additives. The block polymerization was used, e.g., short PE chains were introduced into the long PP ones. Nonisothermal crystallization from molten material allows simulating injection processing, the method used to obtain the material, better than the isothermal regime. In our case, industrial samples (A, B, C, D) differed in the additives used (antioxidant, anti-UV, and coloring). Some of them (A and B) were subjected to artificial aging in a Xenotest 450 chamber with a xenon-arc lamp to simulate the effects of natural radiation. As the aging time simulated was 5000 h, they were labeled as A-5000 h and B-5000 h, which corresponds to 2.5 years of natural aging. Moreover, we analyzed the samples not aged, labeled as A, B, C, and D.

Next, samples of approximately 5 mg were encapsulated in aluminum differential scanning calorimetry (DSC) pans and measurements were performed using a Mettler TA4000 thermo-analizer coupled with a low temperature DSC 30 calorimeter. The instrument was previously calibrated with indium, lead, and zinc standards. Sample heating was at a 10 K/min rate. Each sample was then cooled at 2.5, 5, 10, 20, and 40 K/min. In other words, kinetics is studied from cooling experiences. Figures 1 and 2 show the DSC curves corresponding to samples A and B at different cooling rates.

The microstructure of samples was characterized by scanning electronic microscopy (SEM) in a Zeiss DSM 960A apparatus. Resolution was 3.5 nm, acceleration voltage was 15 kV, and working distance was between 10 and 20 mm. Samples had been sputtered previously with K 550 Emitech equipment. The aim is to observe microstructure changes resulting from the degradation phenomena related to aging processes as well as the effects of the thermal treatments applied to the material.

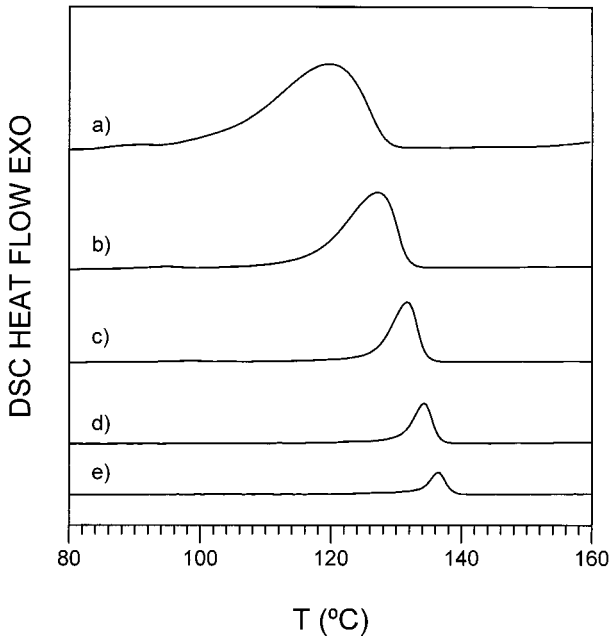

Figure 2 DSC curves corresponding to sample B cooling at different rates: (a) −40 K/min, (b) −20 K/min, (c) −10 K/min, (d) −5 K/min, and (e) −2.5 K/min.

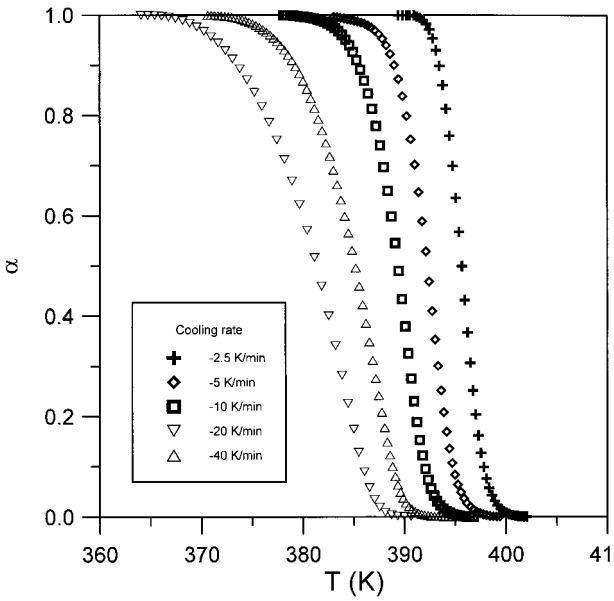

Figure 3 Sample A-5000 h transformed fraction versus temperature at different cooling rates.

RESULTS AND DISCUSSION

Determining surface superficial energy is one of the most characteristic methods to describe the crystallization of previously molten polymers. Such energy, σ, is formed by lateral surface energy, σ_l, and by end surface energy, σ_e. The first corresponds to the nondeformed part of the polymer's lamellae structure, whereas the latter is released by the ridged surface perpendicular to the axis of the polymeric chain.[12,13] That is to say, $\sigma^3 = \sigma_l^2\sigma_e$.[14]

Using eq. (1), the transformation rate, $d\alpha/dt$, becomes the following expression:

$$d\alpha/dt = nk^{1-n}f(\alpha) \tag{3}$$

where $f(\alpha)$ follows the JMAE model, $f(\alpha) = (1 - \alpha)\,[\ln(1 - \alpha)]^{-(n-1)/n}$. The representation of the transformed fraction versus temperature (see Figs. 3 and 4) depicts samples A-5000 h and B-5000 h curves corresponding to the different cooling experiences. In nonisothermal processes with a constant cooling rate, β, the relation between variables t and T is given by $\beta = -dT/dt$. If we apply eq. (3), variables α and t (or T) are separated:

$$\int_0^{\alpha_p} \frac{d\alpha}{f(\alpha)} = n\int_0^{\Delta T_p} k^{1/n}\frac{dT}{\beta} = n\int_0^{t_p} k^{1/n}\,dt \tag{4}$$

where ΔT_p is the undercooling with respect to melting temperature, T_m, where the curve $d\alpha/dt$ reaches its maximum value, α_p. T_p and t_p are, respectively, the temperature and the time at which α_p is obtained. Taking into account that bi- or three-dimensional nucleation is always present in crystalline polymer,[15] in the bi-dimensional case, eq. (4) can be rewritten as follows:

$$\int_0^{\alpha_p} \frac{d\alpha}{f(\alpha)} = n\int_0^{t_p} \exp\left[-\frac{L}{(\beta t)}\right] dt \tag{5}$$

In the three-dimensional one as:

$$\int_0^{\alpha_p} \frac{d\alpha}{f(\alpha)} = n\int_0^{t_p} \exp\left[-\frac{M}{(\beta t)^2}\right] dt \tag{6}$$

Terms L and M are given by the following expressions:

$$L = \frac{4a_0\sigma_l\sigma_e V_m}{\Delta S_m k T_m} \tag{7}$$

and

$$M = \frac{16}{3}\,\pi\,\frac{\sigma_l^2\sigma_e V_m^2}{\Delta S_m^2 k T_m n} \tag{8}$$

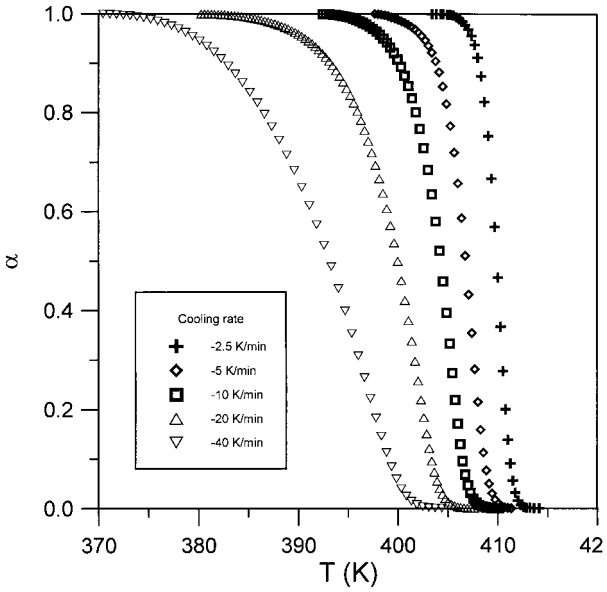

Figure 4 Sample B-5000 h transformed fraction versus temperature at different cooling rates.

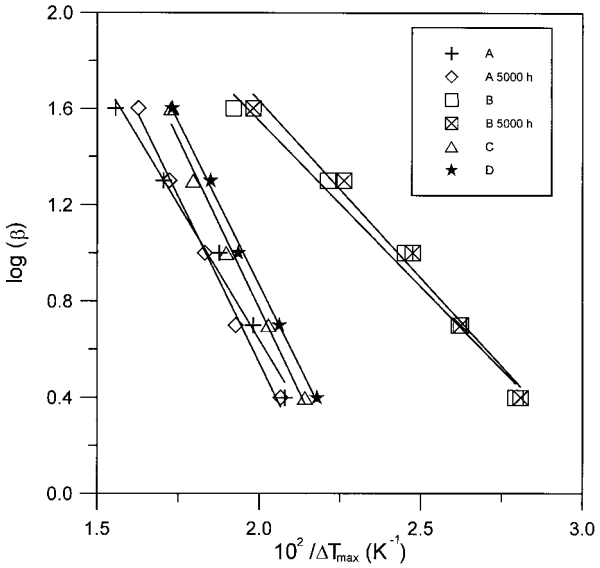

Figure 5 $\ln(\beta)$ versus $1/\Delta T_p$ for the different samples.

where V_m is the molar volume of the crystallizing material, ΔS_m is melting entropy, and a_0 is the crystalline network parameter. For the material here analyzed, PP–PE, the value of these parameters was[15]: $V_m = 28$ cm^3 mol^{-1}, $\Delta S_m = 23.5$ JK^{-1} mol^{-1}, and $a_o = 3.596\ 10^{-8}$ cm. The approximate solution of eqs. (5) and (6) results in the following relationships:

$$\log(\beta) = N - [L/(2.3\Delta T_p)] \tag{9}$$

and

$$\log(\beta) = P - [M/(2.3\Delta T_p^2)] \tag{10}$$

where N and P are constant. The graphical representation of $\log(\beta)$ versus $1/\Delta T_p$ or $1/\Delta T_p^2$ supplies us with parameters L and M from slope (see Figs. 5 and 6). Once these parameters are calculated, their coefficient allows the calculation of σ_l; and σ_e follows readily. To calculate surface energies, $n = 3$ have been utilized.[16] Table I contains the values obtained for the different parameters. The values of σ ranged from 17.3 to 23.6 kJ · m^{-2}. Bibliographic references on PP-based copolymers have similar values, as 18.5 kJ · m^{-2},[17] 18.1 kJ · m^{-2}.[18] Differences should be attributed to the use of different additives and not to the aging degree of samples. The artificial aging is responsible for a slight increase of σ values (i.e., increase of 1.6 kJ · m^{-2} for sample A and 0.3 kJ · m^{-2} for sample B). On the other hand, the σ value of sample B is considerably lower than that of samples A, C, and D. Therefore, the nature of additives greatly influences the σ values.

Our microstructure study was aimed at visualizing the difference between aged and nonaged samples. The study of the superficial zone only allows stating, in some zones, the presence of different impurities and a nonsmooth surface. Concerning other zones, the naturally aged and the nonaged (micrographs 7(a) and 7(b) corresponding to sample D) had a smooth and striated surface tracing in the initial lamella shape. The aging process turned it into a structure in which the surface was broken and a new roof-shaped structure was created.

Moreover, we also performed fracture essays in liquid nitrogen. Thus, we realized that sample B was less resistant to fracture, which implies a lower initial flexibility of this sample. We probed it several times; original sample B has a different mechanic behavior. When the fractured zone was analyzed for both aged and nonaged samples, no apparent microstructure difference could be observed. Hence, the conclusion was that degradation and aging only affects appreciably the superficial zone. The micrographs on Figures 8(a) and 8(b) correspond to the fractured zone of samples A and A-5000 h.

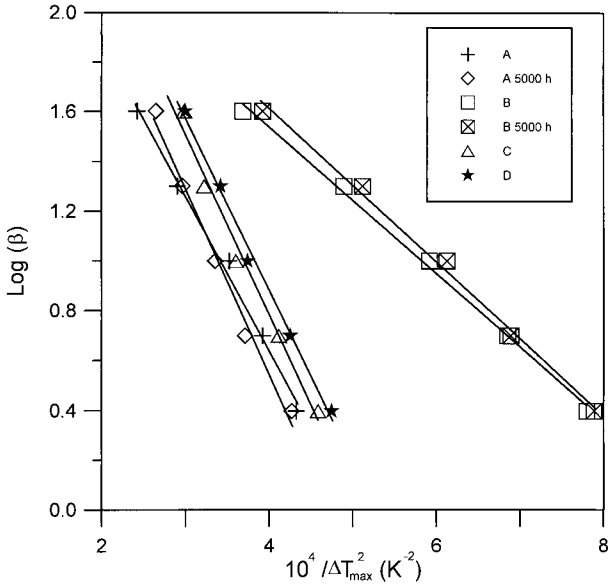

Figure 6 $\ln(\beta)$ versus $1/\Delta T_p^2$ for the different samples.

Table I Kinetic Parameters M and L Calculated from the Slope of Charts on Figures 5 and 6, and Specific Surface Energies (kJ · m^{-2})

Sample	M (K^2)	L (K)	σ_l (kJ · m^{-2})	σ_t (kJ · m^{-2})	σ (kJ · m^{-2})
A	14200 ± 350	515 ± 35	6.0 ± 0.6	310 ± 50	22.3 ± 1.3
A-5000 h	17100 ± 500	635 ± 25	5.8 ± 0.6	390 ± 55	23.6 ± 1.4
B	6750 ± 100	315 ± 25	4.6 ± 0.5	245 ± 45	17.3 ± 1.3
B-5000 h	7100 ± 150	340 ± 10	4.5 ± 0.3	270 ± 25	17.6 ± 0.8
C	16750 ± 600	650 ± 40	5.6 ± 0.7	410 ± 55	23.4 ± 1.7
D	15200 ± 350	610 ± 20	5.5 ± 0.6	395 ± 55	22.8 ± 1.4

CONCLUSIONS

Nonisothermal solidification process of PP–PE-based copolymers with different additives was analyzed by DSC. Specific surface energies were calculated by the Dobreva method. The σ values of all samples ranged from 17.3 to 23.6 kJ · m^{-2}. These values are similar to those reported in the references. In the different parameters calculated, the use of different industrial additives plays a more important role than the artificial

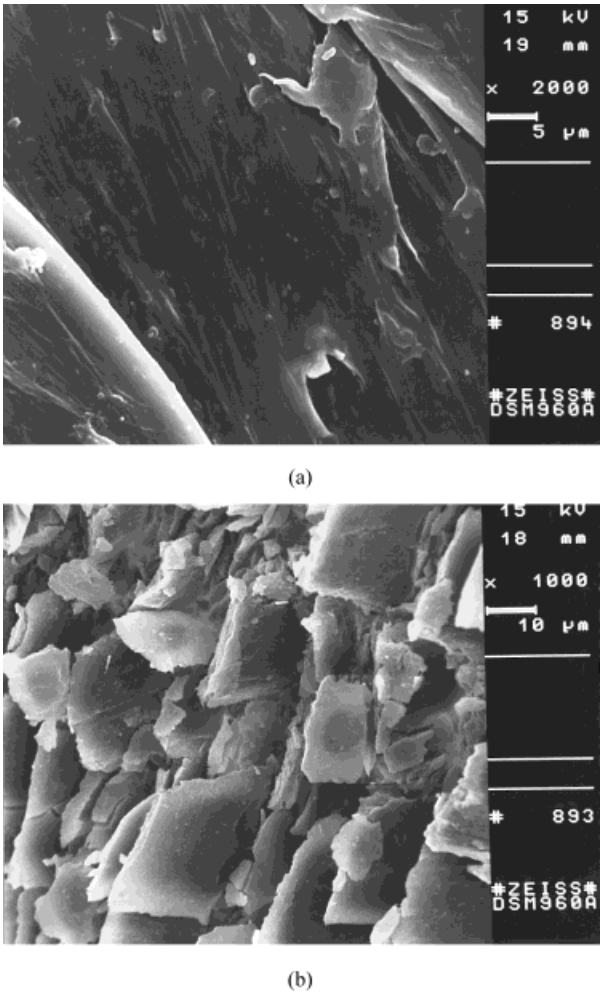

Figure 7 Micrographs corresponding to the superficial zone of: (a) nonaged sample D, and (b) sample D after 2.5 years of natural aging.

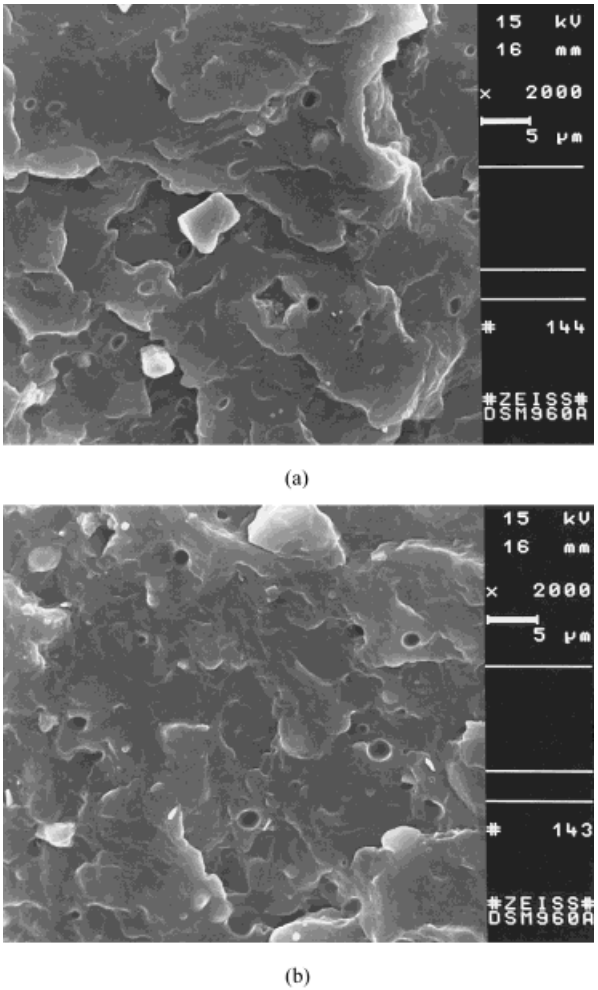

Figure 8 Micrographs after samples' internal zone fracture: (a) A and, (b) A5000 h.

aging applied to several samples. The artificial aging is responsible for a slight increase of σ values (i.e., increase of 1.6 $kJ \cdot m^{-2}$ for sample A and 0.3 $kJ \cdot m^{-2}$ for sample B). On the other hand, the σ value of sample B is considerably lower than that of samples A, C, and D (i.e., 17.3 $kJ \cdot m^{-2}$ for sample B vs an average value of 23.0 $kJ \cdot m^{-2}$ for the other samples).

From microstructure analysis, aging only affects superficial zones because no changes in the morphology of the central zone were detected in the different samples. Sample B shows a different behavior; it was less resistant to fracture. From DSC and SEM measurements, we can state the additive influence on the original sample behavior as well as on the solidification process of PP–PE-based copolymers.

REFERENCES

1. Ozawa, T. Polymer 1971, 12, 150.
2. Sesták, J. In Comprehensive Analytical Chemistry; Turi, E. A., Ed. Academic Press: New York, 1981; p. 435.
3. Zhang, M.; Zeng, H.; He, Y.; Mai, K. Termochim Acta 1995, 257, 183.
4. Suñol, J. J. Ph D Thesis, Universitat Autònoma de Barcelona, 1996.
5. Avrami, M. J. Chem Phys 1939, 7, 1103.
6. Kolmogorov, A. Izv Acad Nauk USSR Ser Math 1937, 1, 355.
7. Chen, H. C. J Non-Cryst Solids 1978, 27, 257.
8. Brown, W. E.; Dollimore, D.; Galwey, A. K. In Comprehensive Chemical Kinetics; Bamford, C. H.; Tipper, C. F. H., Eds. Elsevier: Amsterdam, 1980; Vol. 22; p. 115.
9. Clavaguera, N.; Saurina, J.; Lheritier, J.; Masse, J.; Chauvet, A.; Mora, M. T. Thermochim Acta 1997, 290, 173.
10. Dobreva, A.; Gutzow, I. Cryst Res Technol 1990, 25, 927.
11. Dobreva, A.; Alonso, M.; Gonzalez, M.; Gonzalez, A.; de Saja, J. A. Termochim Acta 1995, 258, 197.
12. Flory, P. J. J Chem Phys 1949, 17, 223.
13. Mandelkern, L. J Appl Phys 1955, 26, 443.
14. Gutzow, I.; Dochev, V.; Pancheva, E.; Dimov, K. J Polym Sci Polym Phys 1978, 16, 1155.
15. Price, F. In Nucleation; A. C. Zettlemoyer: New York, 1969; Chapter 8.
16. Khunova, V.; Smatko, V.; Hudec, I.; Beniska, J. Prog Colloid Polym Sci 1988, 78, 188.
17. Dobreva, A.; Gutzow, I. Cryst Res Technol 1991, 26, 863.
18. Monasse, B.; Haudin, J. M. Colloid Polym Sci 1986, 264, 117.